Performance of the BeOSL eye lens dosemeter with radiation protection glasses

Article *in* Radiation Measurements · December 2019

DOI: 10.1016/j.radmeas.2019.106235

CITATIONS
6

READS
132

13 authors, including:

Vedran Bandalo
Mirion Technologies (AWST) GmbH
12 PUBLICATIONS **162** CITATIONS
SEE PROFILE

Markus Figel
Helmholtz Zentrum München
43 PUBLICATIONS **404** CITATIONS
SEE PROFILE

Matthias Greiter
Quart GmbH
36 PUBLICATIONS **294** CITATIONS
SEE PROFILE

J. Brönner
Mirion Technologies (AWST) GmbH
14 PUBLICATIONS **44** CITATIONS
SEE PROFILE

Performance of the BeOSL eye lens dosemeter with radiation protection glasses

V. Bandalo[1]*, M. Figel[1], M. Greiter[1], J. Brönner[1], P. Kleinau[1], T. Haninger[1], I. Strobel[1], E. Mende[1], P. Scheubert[2], R. Eßer[2], M. Furlan[3], M. Schmid[4], H. Hoedlmoser[1]

[1]Helmholtz Zentrum München, Individual Monitoring Service, Munich, Germany

[2]Dosimetrics GmbH, Munich, Germany,

[3]Dosilab AG, Köniz, Switzerland, [4]MAVIG GmbH, Munich, Germany

This is the submitted version of the article. It has been **extensively** edited, including addition of new data, during the review process!

The final version was published by Radiation Measurements and can be found at the following DOI: https://doi.org/10.1016/j.radmeas.2019.106235

The final version was published by Radiation Measurements and can be found at the following DOI: https://doi.org/10.1016/j.radmeas.2019.106235

Performance of the BeOSL eye lens dosemeter with radiation protection glasses

V. Bandalo[1]*, M. Figel[1], M. Greiter[1], J. Brönner[1], P. Kleinau[1], T. Haninger[1], I. Strobel[1], E. Mende[1], P. Scheubert[2], R. Eßer[2], M. Furlan[3], M. Schmid[4], H. Hoedlmoser[1]

[1]Helmholtz Zentrum München, Individual Monitoring Service, Munich, Germany

[2]Dosimetrics GmbH, Munich, Germany,

[3]Dosilab AG, Köniz, Switzerland, [4]MAVIG GmbH, Munich, Germany

Abstract

A new BeOSL eye lens dosimeter for integration in radiation protection glasses has been investigated in laboratory tests with an Alderson head phantom. The results show both the measurement capabilities of the dosemeters and the protective effect of the glasses. Different measurement positions behind glasses have been compared to the standardized wearing position realized in MAVIG BR330 featuring an integrated dosemeter fixation. Results confirm the choice of a measuring position behind the side shielding next to the eye closer to the radiation source. Results are supplemented by data from Monte Carlo Simulations.

Key words extremity dosimetry, eye lens, OSL, BeO, radiation protection glasses, BeOSL

1 Introduction

The Individual Monitoring Service (IMS) at the Helmholtz Zentrum München has introduced a new BeOSL eye lens dosemeter [1] (ELD) for use with a new mechanical interface for the integration in radiation protection glasses (RPG) developed in a collaboration with MAVIG GmbH and Dosilab AG. The ELD uses the new BeOSL detector element for extremity dosimetry [1], [2], which is based on the BeOSL technology used in whole body dosimetry [3]. The ELD has been submitted to PTB Braunschweig for certification as an official personal dosemeter for photon radiation in Germany. In the meantime, several customers of the IMS already use the ELDs to investigate certain work places, mainly in interventional radiology. For these studies it is very important to know the dosimetric performance of the ELD with and without the use of RP glasses. The work in [1] has investigated the performance of the ELD without the glasses in the standardized calibration settings according to ISO 4037 [4]-[6] showing conformity with the requirements of PTB and IEC [7]. In the ongoing clinical studies it is, however, even more important to know the dosimetric behaviour of the ELD in combination with RP glasses. Therefore, we investigate the performance of

The final version was published by Radiation Measurements and can be found at the following DOI: https://doi.org/10.1016/j.radmeas.2019.106235

ELDs placed inside RP glasses, using an Alderson head phantom, to show the shielding efficiency of the lead glasses and the variation due to positioning. The following issues are addressed in the investigation:

- At first we establish a reference for our measurements by comparing the performance of the ELD on the Alderson head phantom to the standard calibration settings on the ISO cylinder phantom.
- Next, we investigate the response of ELDs fixed to the inside of the new BR330 glasses compared to multiple other measurement locations behind the glasses, e.g. positions directly on both eyes of the phantom. We use the measurement without glasses as the baseline.
- We also compare the BR330 to other MAVIG RPG models and to one RP visor and one model of standard laboratory protective eyewear (non-RP).
- As some of our customers are interested in performing measurements with ELDs fixed both to the inside and to the outside of their glasses for workplace characterization, we also investigated differences between ELDs positioned on the outside of glasses to ELDs directly on the phantom head without glasses.
- Finally, we performed simulations with a Monte Carlo (MC) model using a simplified geometry of a cylinder phantom and a planar 0.5 mm lead shield for photon energies from 10 to 1250 keV. We investigate whether we can predict the BR330 performance over the full photon energy range with a limited number of measurements with different radiation qualities.

2 Materials and Methods

2.1 Irradiations

All dosimetric tests were carried out in the secondary standard irradiation facilities of the IMS in Munich [8], [9], [10]. Calibration procedures in these labs are in accordance with the recommendations of the ISO 4037 [4]-[6] series. All x-ray irradiations were performed with nominal $H_p(3)$ doses based on conversion coefficients for the ISO cylinder phantom. Irradiations were carried out at a 2 m distance. Effects of the protective glasses and changes in geometry were determined in relative measurements, i.e. by normalizing the measured doses behind protection equipment to the dose measured on the eye of the head phantom in the unprotected case. The nominal doses, usually 3 mSv but up to 30 mSv in certain cases, were chosen to ensure high enough signal, on the dosemeters so that additional uncertainty due to

The final version was published by Radiation Measurements and can be found at the following DOI: https://doi.org/10.1016/j.radmeas.2019.106235

the read-out system would be minimised. Finally, in the majority of tests H-60 and N-80 radiation qualities were used, as they cover the most commonly used energy range in radiology, with a small selection of cases also including N-150. Beta response to $^{90}Sr/^{90}Y$ was tested in a PTB beta standard BSS 2 [11]. The majority of radiation qualities and positions had between 5 and 10 dosemeters irradiated and evaluated. The arithmetic mean of the individual dosemeter results was used as the measured dose value while the expanded uncertainty with coverage factor of 95% was used for the error bars.

2.2 Radiation protection glasses, adapters and phantoms

The main emphasis of our investigations was the new MAVIG RPG model BR330 with the integrated mechanical interface for ELDs [1]. Additionally, MAVIG RPG Models BR115, BR126, BR310, BR322, BR330, BR331, MAVIG BRV501 visor [12], and a pair of plastic laboratory glasses, were used with ELDs in adhesive adapters [1]. All investigations with RPGs were performed on an Alderson-Rando head phantom. For comparison to standardized calibration conditions the ISO head cylinder phantom was used.

Figure 1 Alderson-Rando head phantom equipped with dosemeters on eyes and temple for baseline irradiations. Laser lines aid in positioning of the phantom in the beam centre and at the distance of 2 m.

Irradiations were structured so that for each angle and radiation quality a combination of four ELDs, left/right eye and left/right phantom temple, were exposed without any protection in order to establish the baseline dose, see Figure 1. This was followed by exposure of ELDs with an identical nominal dose in various positions, using the protective equipment, see Figure 2. The positions used for the ELDs were: left/right eye, left/right phantom temple emulating the use of the headband adapter [1] behind the RP glasses, and ELDs mounted behind the shielding on both sides of the glasses. Additionally, two different 3D printed

The final version was published by Radiation Measurements and can be found at the following DOI: https://doi.org/10.1016/j.radmeas.2019.106235

prototype clip-on adapters, type A and type B, were used attached to the temple of the glasses to estimate the unshielded dose. It should be noted that the used clip-on adapters had different shapes. The adapter pointing towards the phantom would position the ELD behind the temple of the glasses, which can influence the detected dose depending on the material.

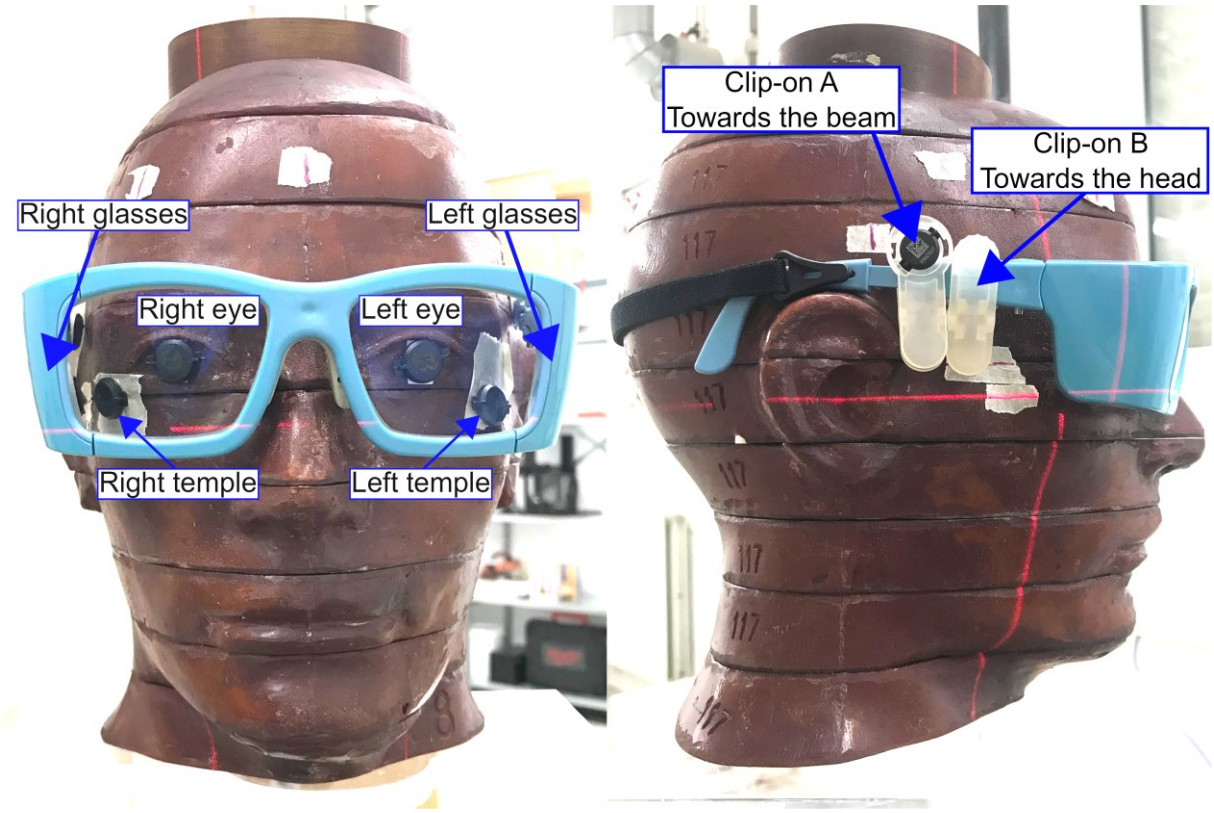

Figure 2 ELD positions used during the evaluation of radiation protection glasses, here shown with the BR330 model.

Figure 3 shows the various types of protection equipment on the phantom head. Table 1 summarises their protective properties. Beta irradiations were performed with the same approach and ELD positions, but with only BR330 radiation protection glasses and the laboratory glasses as a comparison.

The final version was published by Radiation Measurements and can be found at the following DOI: https://doi.org/10.1016/j.radmeas.2019.106235

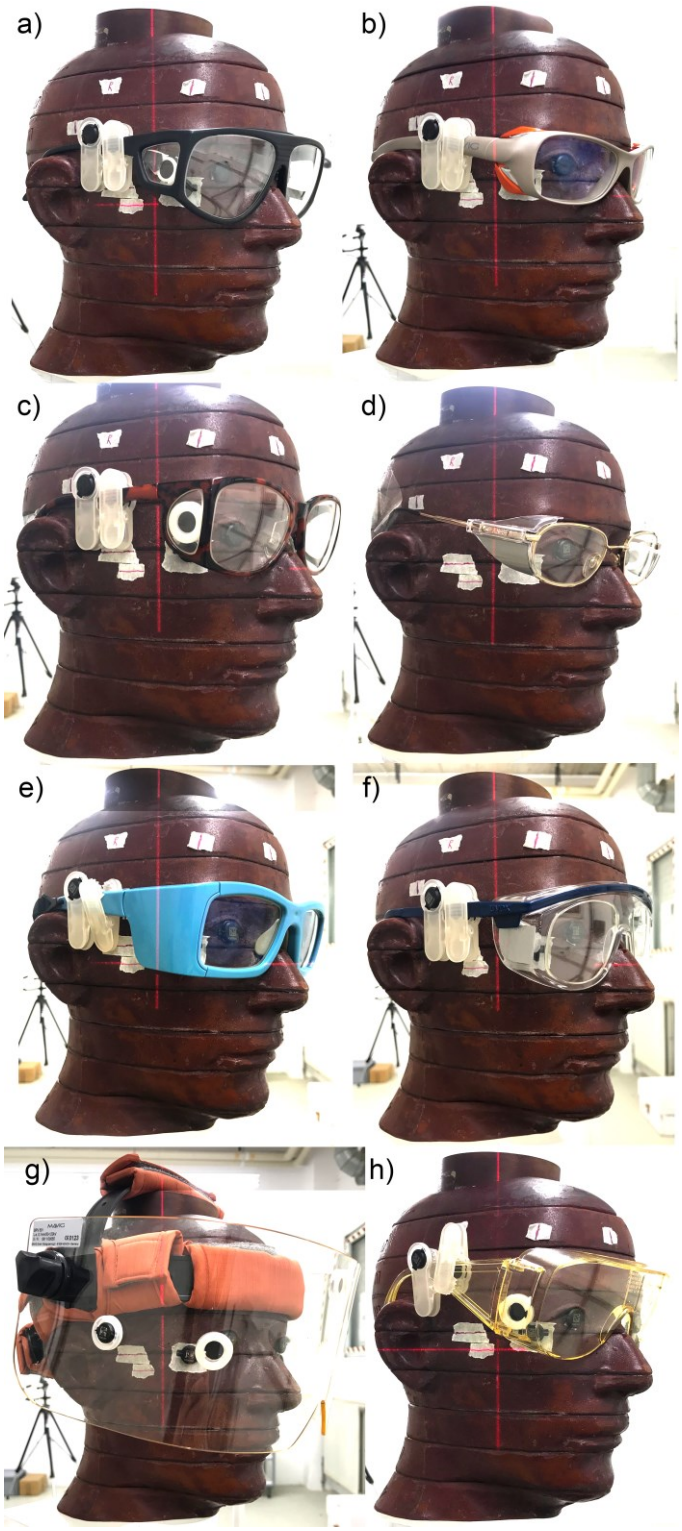

Figure 3 Image of all the protective equipment used on the phantom. The glasses imaged are: a) BR115, b) BR126, c) BR310, d) BR322, e) BR330, f) BR331, g) BRV501 visor, and h) laboratory protection glasses.

The final version was published by Radiation Measurements and can be found at the following DOI: https://doi.org/10.1016/j.radmeas.2019.106235

Glasses model	Front shielding mm Pb equivalent	Side shielding mm Pb equivalent
BR115	0.75	0.75
BR126	0.50	0.50
BR310	0.75	0.75
BR322	0.75	0.50
BR330	0.50	0.50
BR331	0.75	0.50
BRV501 (Visor)	0.10	0.10
Laservision skyline	2.8 mm plastic	2.8 mm plastic

Table 1 List of all radiation protection equipment tested and their shielding properties from the front and the sides. Note: Laservision skyline is not an RPG. It was included for comparison only.

2.3 Monte Carlo Simulations

The radiation transport code MCNP6 [13] was used to model simplified photon irradiation geometries on the ISO cylinder phantom with and without a 5 cm x 10 cm x 0.5 mm Pb shield. The energy response of the ELDs was obtained from multiple simulation runs with monoenergetic photons as described in [14]. To obtain correct results in connection with the lead shielding, it was necessary to include electron transport throughout the geometry. Examples of the irradiation geometries are shown in Figure 10 and described in section 3.5.

3 Results

3.1 Alderson phantom vs cylinder phantom

A comparison of ELDs exposed to identical nominal $H_p(3)$ doses on the cylinder phantom and on the Alderson phantom was carried out to investigate differences in the backscatter contributions to the dose due to the difference in volume and material composition of the two phantoms. For the irradiation on the Alderson phantom, the ELDs were placed on the temple of the head. The head was rotated to ~ 45°, making the angle of incidence on the ELD 0° and thus identical to the irradiation on the cylinder phantom. The measurements on the Alderson phantom delivered on average 93% of the dose on the cylinder phantom, mainly due to phantom geometry differences. This reduction was found to be very similar for the three investigated radiation qualities – see Figure 4.

The final version was published by Radiation Measurements and can be found at the following DOI: https://doi.org/10.1016/j.radmeas.2019.106235

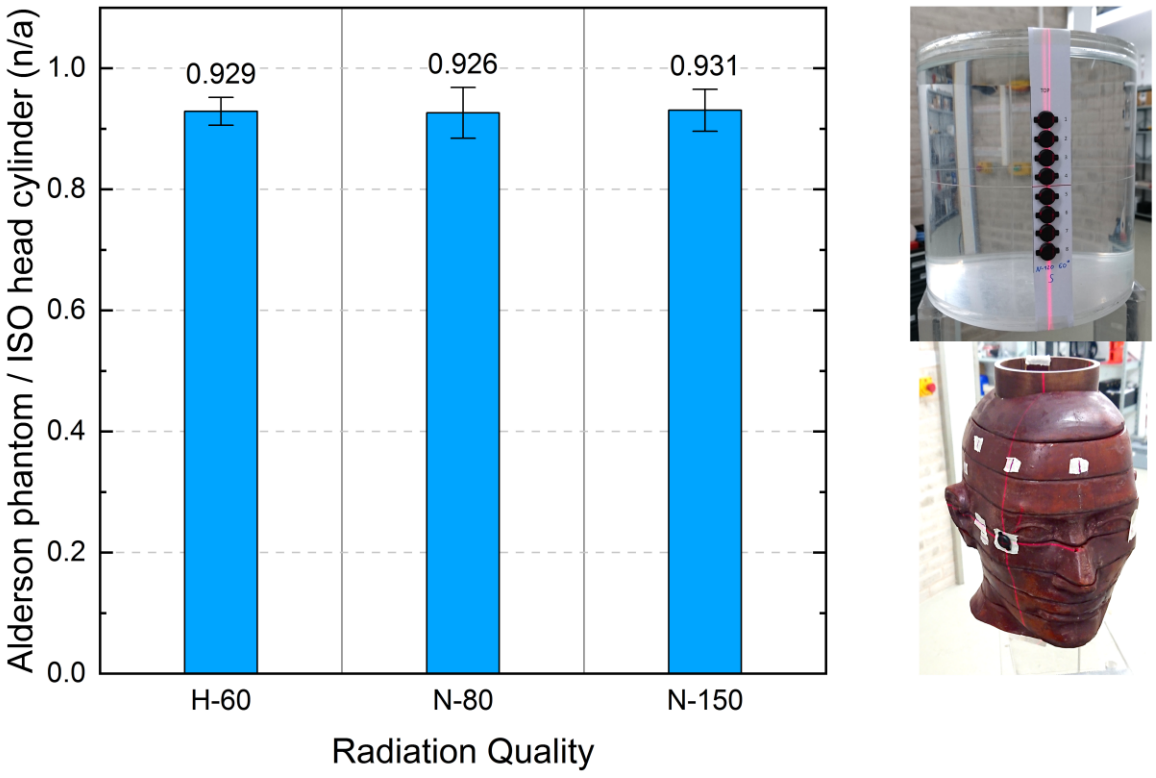

Figure 4 Comparison of irradiation of ELDs on the Alderson phantom with irradiations on the cylinder phantom. Left and right pictures show the irradiation geometries on the two phantoms and the graph shows the ratio of the measured values for the investigated radiation qualities.

3.2 Measurements with BR330 glasses

3.2.1 BR330 evaluation

The evaluation of the BR330 RPGs was performed using H-60, N-80, and N-150 radiation qualities with the phantom rotated to a 45° angle and with the right side of it towards the source. The measurements with BR330 were repeated ten times each, while the number of measurements without protection was 6 for H-60, 1 for N-80, and 7 for N-150. The results are shown in Figure 5 with all doses normalised to the dose for the unprotected right eye for the respective radiation quality and error bars showing the 95% confidence interval.

The final version was published by Radiation Measurements and can be found at the following DOI: https://doi.org/10.1016/j.radmeas.2019.106235

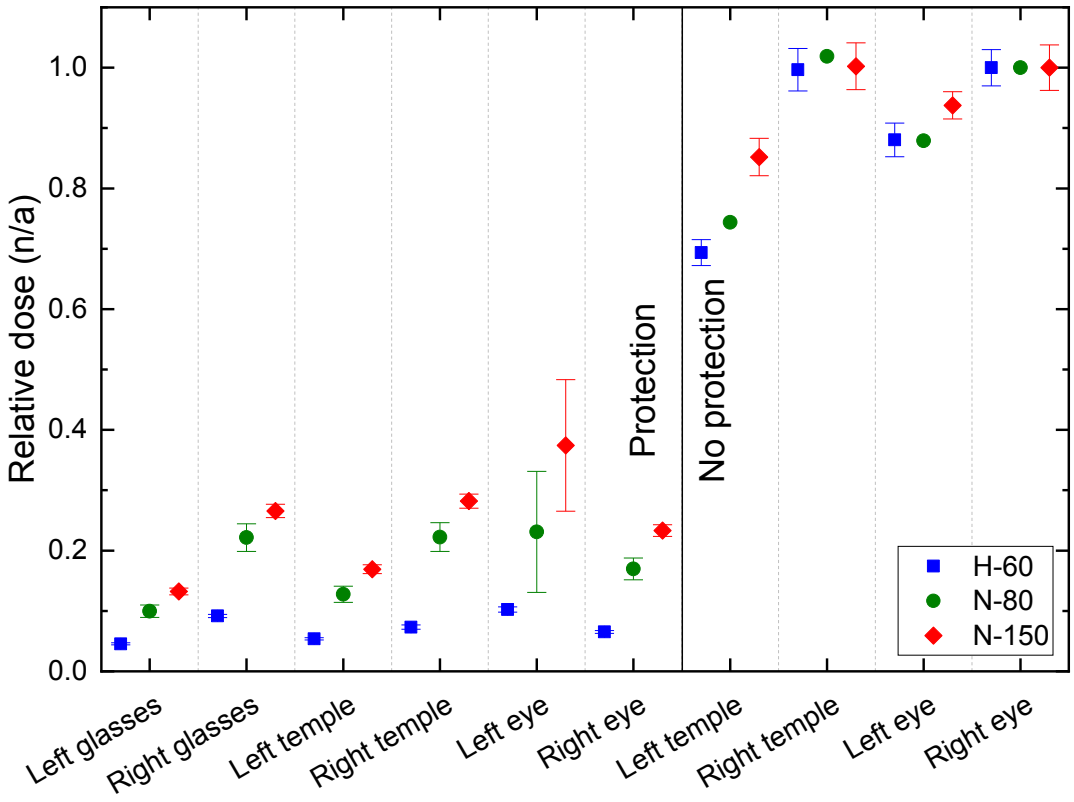

Figure 5 Evaluation of the BR330 radiation protection glasses using H-60, N-80, and N-150 radiation qualities. All values are normalized to the dose received by the ELD placed on the unprotected right eye of the Alderson phantom. Due to a single measurement performed for N-80 without protection there are no error bars on those data points.

The results show the expected protective behaviour with higher levels of protection for lower energies, namely 94% reduction for H-60, 83% for N-80, and 77% for N-150. The values for the right mounting position on the BR330 overestimate the dose by 41% for H-60, 31% for N-80, and 14% for N-150 as compared to the protected right eye dose for their respective radiation qualities. A similar effect is seen for the right temple position, near the right eye, where the overestimation is 12% for H-60, 31% for N-80, and 21% for N-150. Thus, both positions will provide a conservative dose estimate to the lens of the right eye when used with BR330. However, the left eye shows a small decrease in protection as compared to the right eye with the dose reduction compared to the unshielded left eye being 88% for H-60, 74% for N-80, and 60% for N-150. This leads to an underestimation of the dose by up to 10% for H-60, 4% for N-80, and 29% for N-150 when a dosemeter mounted on the right side of the

The final version was published by Radiation Measurements and can be found at the following DOI: https://doi.org/10.1016/j.radmeas.2019.106235

glasses is used. This behaviour is indicative of geometry around the nose area being responsible for the increase of the dose. As there is no shielding close to the nose there is a "leakage" of radiation towards the left eye that will depend on the exact geometry of the RPGs, the user face and the angle towards the source, with higher energy radiation possibly passing through the nose itself.

3.3 Comparison of different RPG models and a visor

In order for a better understanding of geometry effects, as well as the behaviour of different RPGs, we performed a comparison between six RPGs, a visor and laboratory protection glasses. The comparison was performed at a 45° angle with the right side of the phantom towards the source, 2 m distance to the centre of the Alderson phantom, and using H-60, see Figure 6, and N-80, see Figure 7, radiation qualities.

Using RPGs results in a high reduction in dose for both H-60 and N-80 with the ELD mounting position behind the shielding on the right side of the glasses providing a conservative estimate of the eye dose in all cases. The reduction factors were ≈10 for H-60 and ≈5 for N-80. It should be noted that the new BR330 offers better or equal protection at H-60 and N-80 energies for the right eye even though it features less lead equivalent than most of the other glasses. However, the right temple position emulating the use of a headband adapter, was found to be no longer an adequate ELD mounting position, as in several cases it widely overestimates the dose, as this position is not fully protected in some RPG models. This effect is highly dependent on the geometry of the glasses themselves implying that mounting the ELD to the glasses is the preferred position for estimating the dose to the lens of the eye reliably. Depending on the type of glasses that mounting position might be more or less convenient. In the case of the BR126 the adhesive adapter prevents the closing of the glasses for storage. Nevertheless, our findings suggest that optimum ELD mounting position for best estimate of the dose to the lens of the eye is behind the lateral shielding.

Use of the visor simplifies things as it provides shielding for a wide variety of positions while making it simple to estimate the dose by mounting the ELD behind the visor itself. At lower energies, ≤ 60 keV, the visor provides excellent protection. However, at higher energies the 0.1 mm lead equivalent of the visor results in substantially lower shielding as compared to the 0.5/0.7 mm lead equivalent of the RPGs.

The final version was published by Radiation Measurements and can be found at the following DOI: https://doi.org/10.1016/j.radmeas.2019.106235

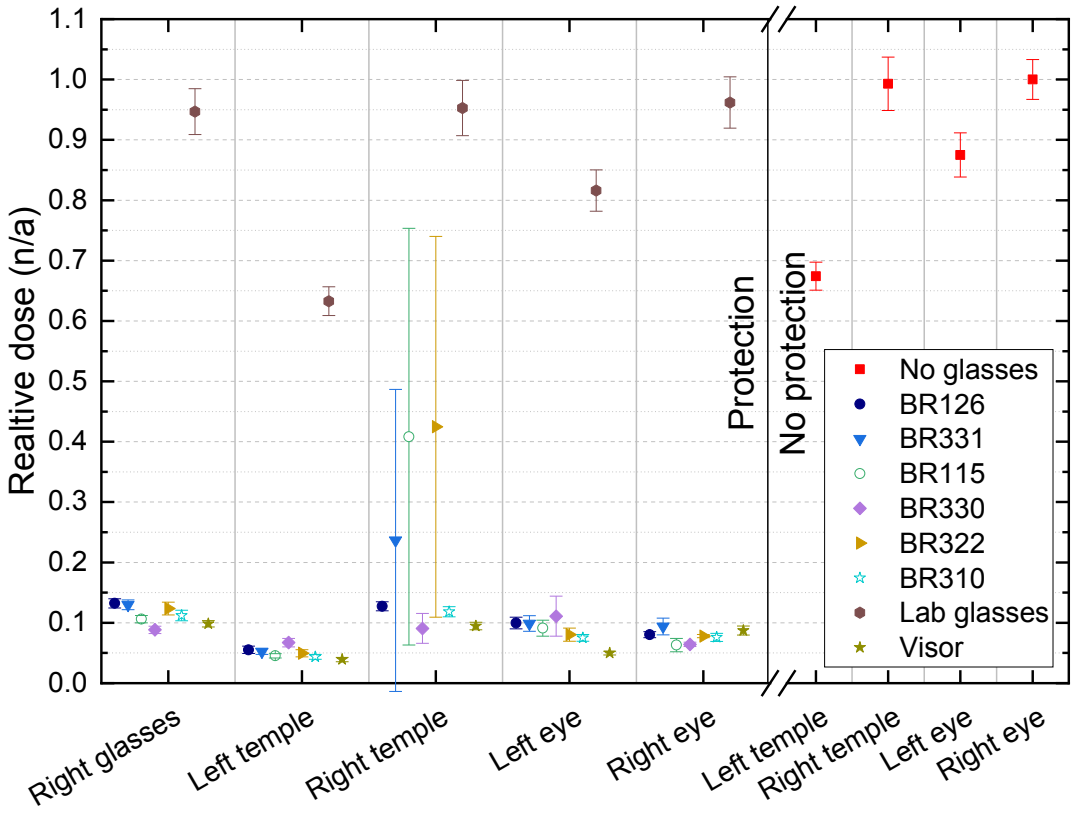

Figure 6 Comparison of radiation protection glasses exposed by H-60. All doses normalised to the unprotected right eye. Error bars show the 95% confidence interval.

The final version was published by Radiation Measurements and can be found at the following DOI: https://doi.org/10.1016/j.radmeas.2019.106235

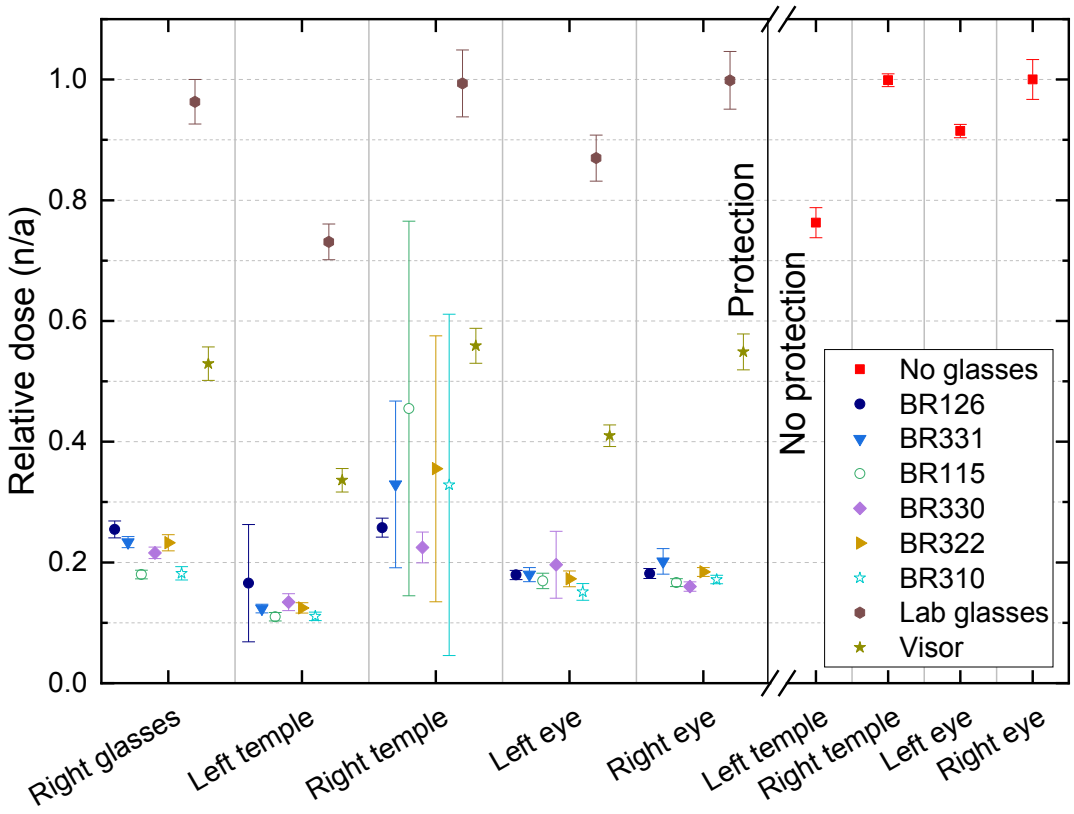

Figure 7 Comparison of radiation protection glasses exposed by N-80. All doses normalised to the unprotected right eye. Error bars show the 95% confidence interval.

3.3.1 Outside glasses vs no glasses

If RPGs or visors are used in work place evaluations, it is sometimes attempted to measure the shielding effect of the glasses by fixing an additional dosemeter to the outside of the glasses and performing a comparison between values measured behind and outside the shielding. While such an approach delivers an approximation of the shielding effect, it significantly affects the dosimetry. The dosemeter fixed to the outside of RPGs is shielded from backscattered radiation from the head and will show smaller dose readings in comparison to an exposure directly on the head without any protection. Therefore, we compared measurements with dosemeters on the outside of BR330 glasses and on the outside of a visor to measurements directly on the unprotected right eye of the phantom, see Figure 8. We found a reduction of 15%-20% for the qualities H-60 and N-80. N-150 irradiations

The final version was published by Radiation Measurements and can be found at the following DOI: https://doi.org/10.1016/j.radmeas.2019.106235

showed much less reduction, as scattering effects are reduced at higher photon energies. For such an evaluation the clip-on adapter A, see Figure 2, is a much better choice, as the backscatter is not shielded and thus provides a correct dose estimate. In the comparison of RPGs the clip-on adapter A gave consistently a 3-9% lower dose as compared to the unprotected eye for various models and energies. The adapter B, in turn, had a very high variability in certain cases due to the unequal shielding by the temple of different glasses.

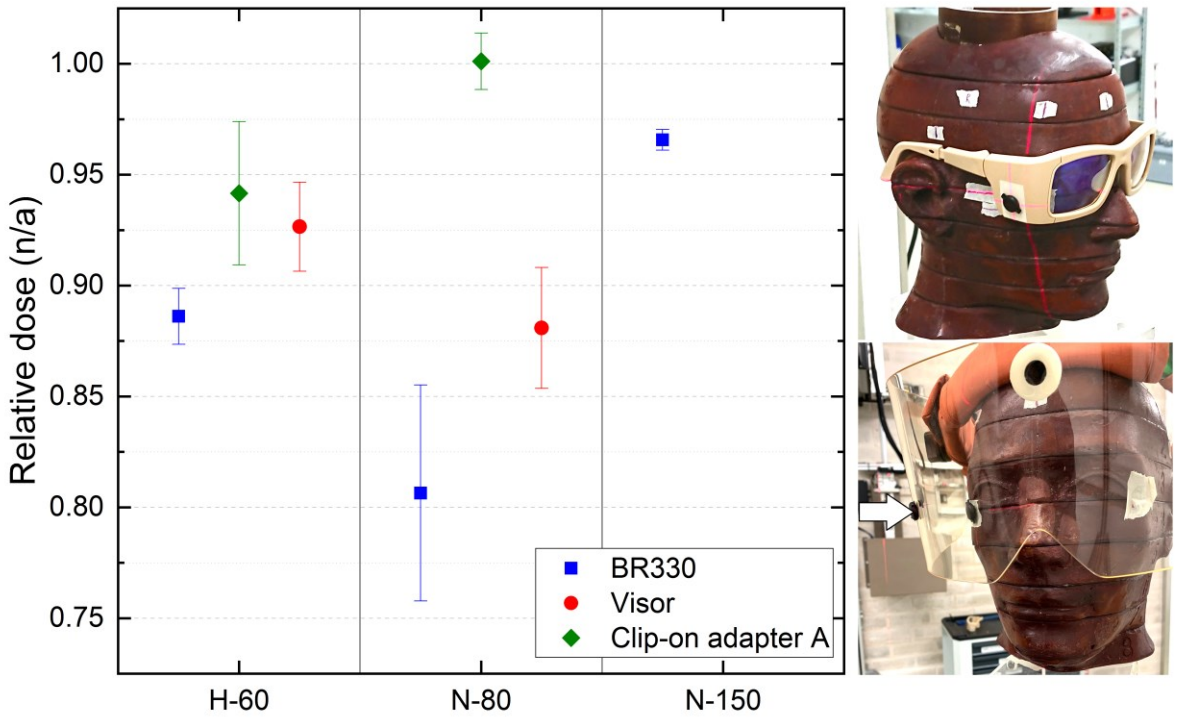

Figure 8 Comparison of irradiations of ELDs on the outside of protective equipment to irradiations of ELDs directly on the phantom without protective equipment. Values outside equipment normalised to the unshielded right eye. Top right image: ELD outside BR330, bottom right image ELD outside visor. For Clip-on adapter A see Figure 2.

3.3.2 Angular dependence BR322 and BR330

Angular dependence of the shielding factor was investigated by comparing the results for BR322 and BR330 radiation protection glasses for angles between 40° and 50° in steps of

The final version was published by Radiation Measurements and can be found at the following DOI: https://doi.org/10.1016/j.radmeas.2019.106235

2.5° in the H-60 radiation field, see Figure 9. The results show that there is a small angle range where shielding of the left eye is decreased from 94% to 89% reduction for BR330 and from 93% to 92% reduction for BR322. Differences between the BR322 and BR330 are due to the geometry and in the case of the lens of the eye due to the distance between the protective glass and the lens. The closer the glass is to the lens, the more area around the lens is covered effectively, thus lowering the susceptibility for "leaking" radiation through the nose area. Comparing BR322 (Fig. 2 d) to BR330 (Fig. 2 e) it is clear that the glass of BR322 is located a lot closer to the eye which compensates for the size difference in the lead glass. This is accompanied by lower shielding performance for the lens of the right eye as more radiation can enter the head close to the eye and scatter towards the lens. In practical applications, the user will move their head and, consequently, the small reduction in protection for certain angles should not impact the total dose to the lens of the eye in any meaningful way.

The final version was published by Radiation Measurements and can be found at the following DOI: https://doi.org/10.1016/j.radmeas.2019.106235

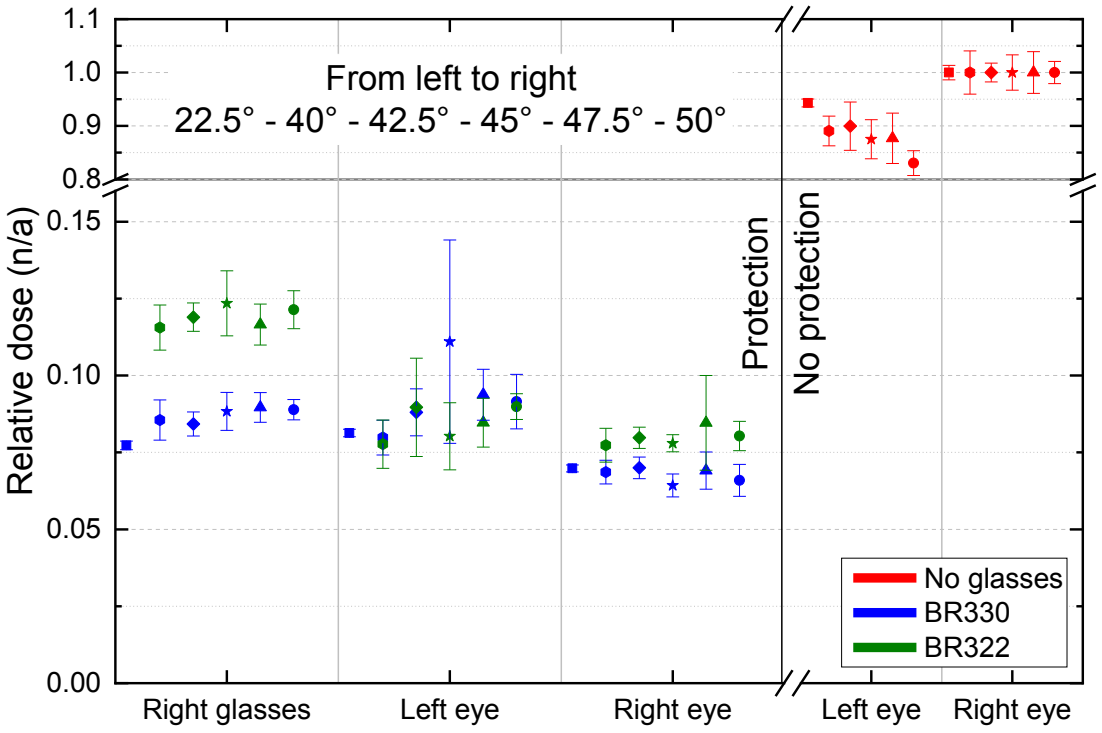

Figure 9 Comparison of measured doses for BR322 and BR330 radiation protection glasses at different angles, 22.5° and 40 to 50° in steps of 2.5°, when exposed to H-60. All doses normalised to the unprotected right eye. Error bars show the 95% confidence interval.

3.4 Beta radiation

For protection against beta radiation we compared the BR330 radiation protection glasses and a pair of laboratory protection glasses in the BSS 2 stand. The laboratory glasses reduce the $H_p(3)$ dose by almost 90% while BR330 reduce it by over 99%. In both cases the protection is sufficient for high energy $^{90}Sr/^{90}Y$ and will be even better for lower energy beta sources.

3.5 Simulation results

The MCNP6 model of the calibration geometry with the ELD on the cylinder phantom, which had been used to obtain the energy response in the development of the ELDs [14], was

The final version was published by Radiation Measurements and can be found at the following DOI: https://doi.org/10.1016/j.radmeas.2019.106235

extended by adding a 5 cm x 10 cm x 0.5 mm lead plate 2 cm in front of the surface of the cylinder phantom. The lead plate is the simplest approximation of the shielding provided by the BR330 RPGs. Several positions of the ELD were investigated in reference to this lead shield. Figure 10 depicts the various geometries, and Figure 11 shows the relative dosemeter readings as a function of photon energy obtained for the various geometries. Figure 11 also compares the simulated data to the measurement results with the Alderson phantom shown above. In the following we present the results for the various geometries using the individual graphs in Figure 11 and the references (a) - (e) in Figure 10:

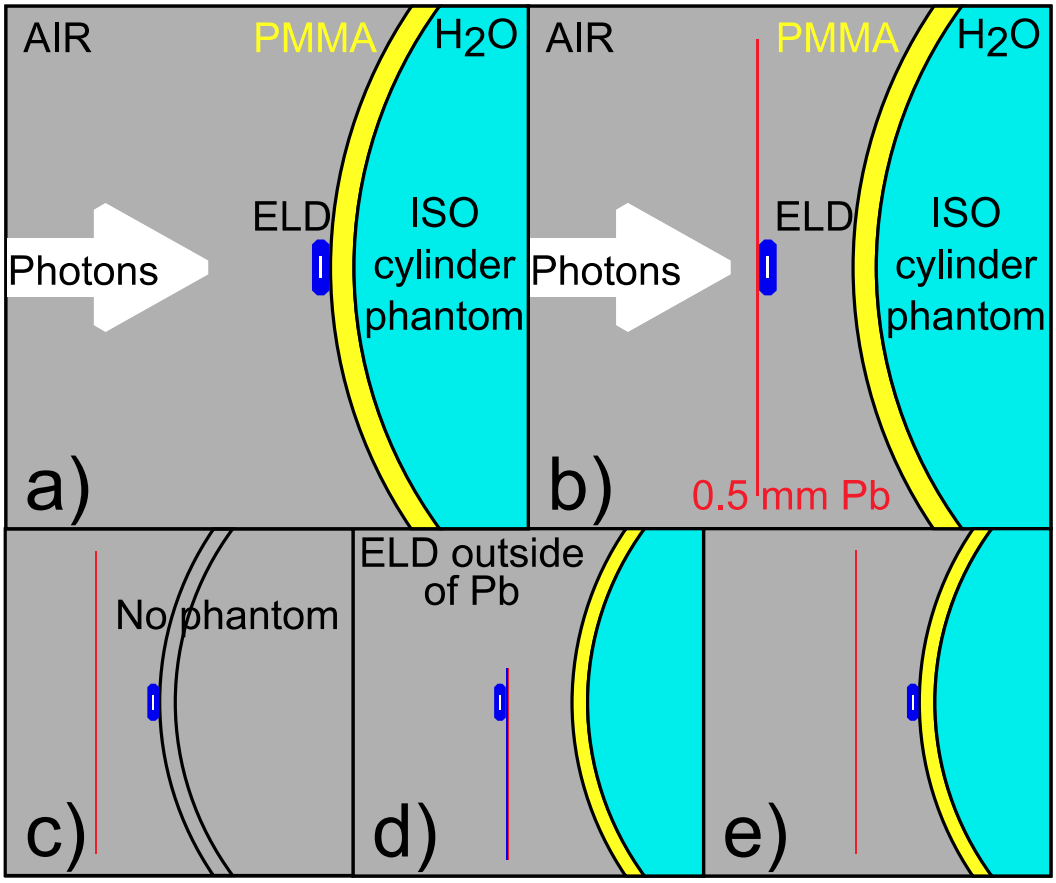

Figure 10 MC Simulation geometries: (a) calibration geometry of ELD on cylinder phantom, (b) approximation of geometry for lead glasses with 0.5 mm lead shield added in front of the phantom and ELD positioned inside the shield, (c) ELD behind lead shield but phantom removed, (d) ELD outside lead shield with phantom present, (e) ELD 2 cm behind lead shield on phantom.

The final version was published by Radiation Measurements and can be found at the following DOI: https://doi.org/10.1016/j.radmeas.2019.106235

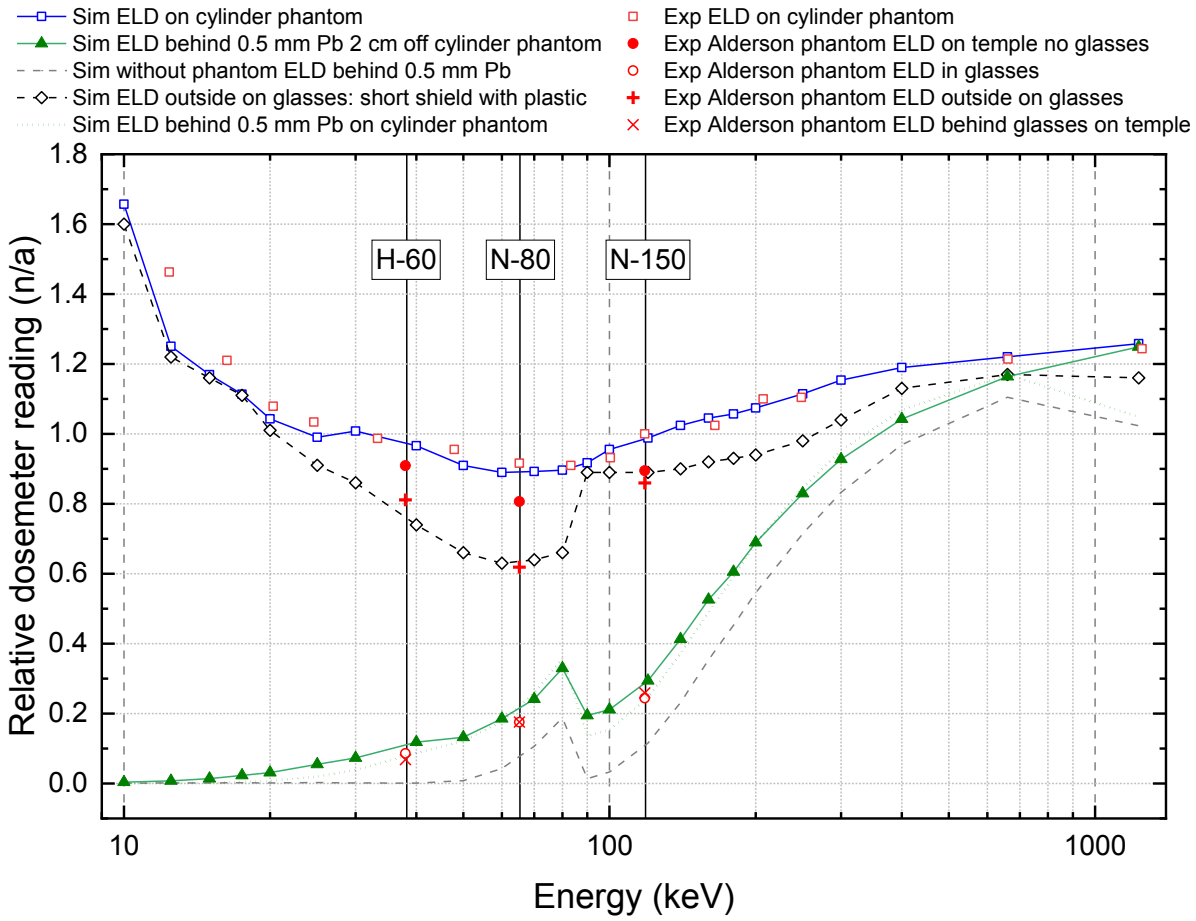

Figure 11 Results for the relative dosemeter readings as a function of photon energy for the various simulation geometries in Figure 10.

(a) Depicts the original calibration geometry with the ELD placed directly on the cylinder phantom. The simulation delivers the energy response of the dosemeter (Figure 11, blue line, open squares) which agrees very well with the experimentally determined response of the ELDs on the cylinder phantom. (Figure 11, red open squares). Note: the ELD system is calibrated at N-150 [1], so the response is equal to 1 at 118.5 keV photon energy. All subsequent simulation results in the additional geometries are relative to this value. Another experimental dataset to compare to is the measurement on the Alderson phantom without RPGs (Figure 11, red full circles): here we find again the small reduction compared to the cylinder phantom reported in section 3.1.

The final version was published by Radiation Measurements and can be found at the following DOI: https://doi.org/10.1016/j.radmeas.2019.106235

(b) In this geometry the 0.5 mm lead shield is introduced 2 cm in front of the phantom and the dosemeter is positioned directly behind the shield. This is the simplest approximation of the situation with the dosimeter mounted in the BR330 RPG, which contains the same 0.5 mm Pb equivalent shielding. The dosemeter reading behind the shield delivered by the simulation (Figure 11, green line and full triangles) shows the expected decrease due to the Pb shield. The shielding effect is increasing with decreasing photon energy. Again the simulated effect is consistent with the measurements using ELDs in the BR330 glasses on the Alderson phantom (Figure 11, red open circles).

(c) In this geometry the phantom is removed. Here the dosemeter reading drops to zero below 40-50 keV (Figure 11, dashed grey line). Therefore we conclude that the residual readings below 40-50 keV in the presence of the phantom (b) are produced by backscattered radiation. The difference between the green line and the grey dashed line is due to the backscatter component of the dosemeter reading.

(d) Here the dosemeter is moved to the outside of the lead shield, corresponding to a measurement with an ELD glued to the outside of RPGs. The geometry is somewhat refined reflecting the asymmetry of the positioning with regard to the edge of the shielding and the additional plastic material in order to better approximate the scattering contributions. The resulting response (Figure 11, dashed black line with open diamonds) again agrees with the results obtained on the RPGs on the Alderson phantom (Figure 11, red crosses) and confirms the underestimation of the unprotected eye lens dose reported in section 3.3.1.

(e) The last geometry investigates possible differences due to the positioning behind the shield. Here the dosemeter is located on the phantom as opposed to (b), where the dosemeter is on the inside of the shield almost 2 cm from the phantom. The resulting graph (Figure 11, green dotted line) agrees well with the result from (b) (Figure 11, green line and full triangles). The corresponding experimental results from exposures with the Alderson phantom, once with the ELD in mounted in the RPGs (Figure 11, red open circles) and once with the ELD on the temple of the phantom (Figure 11, red xs) show the same behaviour in good agreement with the simulation.

4 Summary and Conclusion

We evaluated the behaviour of various radiation protection glasses as well as a visor and laboratory glasses with H-60, N-80, N-150 radiation qualities, and $^{90}Sr/^{90}Y$ beta field. The

The final version was published by Radiation Measurements and can be found at the following DOI: https://doi.org/10.1016/j.radmeas.2019.106235

radiation protection glasses show attenuation of around 90% for H-60, 80% for N-80, 65% for N-150, and 99% for $^{90}Sr/^{90}Y$ in our investigated geometry (source and the phantom head on the same level). This is consistent with previous works in [15][16][17].
We demonstrate that the geometry is a critical factor for the dose evaluation to the lens of the eye. Our results show that the preferred mounting position is behind the lateral shielding of the radiation protection glasses or visor on the side closest to the source. This is consistent with the previous work in [18]. Such positioning of the dosemeter provides a reasonably conservative dose estimate to the lens of both eyes in the majority of practical applications. However, it should be noted that these results depend on correct positioning of the glasses, the user's head and the scatter source in order to ensure that the geometry allows the glasses to actually shield the eyes. Previous works, [19][20][21], have investigated dose reduction factors for various types of RPGs in more realistic scattering geometries. They showed that radiation traveling upwards from the patient can bypass the glasses and reach the eye with a lot less attenuation. Thus, it is vital that radiation protection personnel enforce correct use of protective equipment in order to ensure both protection and correct dose evaluation.

Experimental results have been supplemented with Monte Carlo simulations. Despite the simplified geometry, simulation results are in very good agreement with the experimental results and provide information of the investigated effects over the full photon energy range beyond the three radiation qualities investigated experimentally. They emphasize the importance of the shielding effect of the RPGs in determining the correct eye lens dose.

We hope the results of this investigation help to plan experiments for ongoing and future work place evaluations and evaluations of protective equipment by our customers.

5 References

[1] Hoedlmoser, H., et al, 2019. New Eye Lens Dosemeters for Integration in Radiation Protection Glasses, Radiat. Meas. 125, 106-115.

[2] Scheubert, P., et al, 2019. SSD19, Poster presentation P1-038, http://ssd19.org/poster_presentations/

[3] Haninger, T., Hödlmoser, H., Figel, M., König-Meier, D., Henniger, J., Sommer, M., Jahn, A., Ledtermann, G., and Eßer, R., 2015. Properties of the BeOSL Dosimetry System in the Framework of a Large-scale Personal Monitoring Service, Radiat Prot Dosimetry. https://doi.org/10.1093/rpd/ncv425.

The final version was published by Radiation Measurements and can be found at the following DOI: https://doi.org/10.1016/j.radmeas.2019.106235

[4] ISO 4037-1:2019
[5] ISO 4037-2:2019
[6] ISO 4037-3:2019
[7] IEC 62387:2018, Radiation protection instrumentation - Dosimetry systems with integrating passive detectors for individual, workplace and environmental monitoring of photon and beta radiation.
[8] Bandalo, V., Brönner, J., Greiter, M.B., Hoedlmoser, H., 2018. A Fully Automated Secondary Standard X-Ray Calibration Facility for Personal Dosemeters, accepted for publication by Rad. Prot. Dosimetry. https://doi.org/10.1093/rpd/ncy187.
[9] Greiter, M.B., Denk, J., Hoedlmoser, H., 2016. Secondary Standard Calibration, Measurement and Irradiation Capabilities of the Individual Monitoring Service at the Helmholtz Zentrum München: Aspects of Uncertainty and Automation, Rad. Prot. Dosimetry. https://doi.org/10.1093/rpd/ncv537.
[10] Bandalo, V., Greiter, M. B., Brönner, J., Hoedlmoser, H., 2019. ISO 4037:2019 Validation of Radiation Qualities by Means of Half-Value Layer and $H_p(10)$ Dosimetry, Rad. Prot. Dosimetry, accepted on 2019-08-01. https://doi.org/10.1093/rpd/ncz185
[11] Ambrosi, P., Buchholz, G. and Helmstädter, K., 2007. The PTB beta secondary standard BSS 2 for radiation protection, J. Instrum. 2, p11002.
[12] https://mavig.com/x-ray-protection/eye-protection/ (retrieved on 2019-07-16)
[13] T. Goorley, et al., "Initial MCNP6 Release Overview", Nuclear Technology, 180, pp 298-315 (Dec 2012)
[14] Hoedlmoser, H., et al, 2018. Simulation of OSL and TLD dosemeter response for the development of new extremity dosemeters, Rad. Prot. Dosimetry. https://doi.org/10.1093/rpd/ncy299.
[15] McVey, S, Sandison, A, Sutton, D G, "An assessment of lead eyewear in interventional radiology", J. of Rad. Prot., 33, pp 647-659 (Jun 2013)
[16] Rivett, C, et al., "An assessment of the dose reduction of commercially available lead protective glasses for interventional radiology staff", Rad. Prot. Dosimetry, 172, pp 443-452 (Jan 2016)
[17] Sandblom, V, "Evaluation of Eye Lens Doses Received by Medical Staff Working in Interventional Radiology at Sahlgrenska University Hospital", M.Sc. Thesis Gothenburg Jan 2012

The final version was published by Radiation Measurements and can be found at the following DOI: https://doi.org/10.1016/j.radmeas.2019.106235

[18] Silva, E H, et al., ”Where is the best position to place a dosemeter in order to assess the eye lens dose when lead glasses are used?”, Rad. Meas., 106, pp 257-261 (2017)

[19] van Rooijen, B D, et al., ”Efficacy of Radiation Safety Glasses in Interventional Radiology”, Cardiovasc. Intervent. Radiol., 37, pp 1149-1155 (2014)

[20] Mao, L, et al., “Influences of operator head posture and protective eyewear on eye lens doses in interventional radiology: A Monte Carlo Study”, Med. Phys., 46, pp 2744-2751 (Apr 2019)

[21] Principi, S, et al., “The influence of operator position, height and body orientation on eye lens dose in interventional radiology and cardiology: Monte Carlo simulations versus realistic clinical measurements”, Physica Medica, 32, pp 1111-1117 (Sep 2016)

The final version was published by Radiation Measurements and can be found at the following DOI: https://doi.org/10.1016/j.radmeas.2019.106235